KOM
CORROSION AND MATERIAL PROTECTION JOURNAL

ORIGINAL ARTICLE

sciendo

Impact of the diffusion coefficient calculation on predicting Fe_2B boride layer thickness

El Guerri Y.[1], Mebarek B.[1], Keddam M.[2]
[1] Research Laboratory of Industrial Technologies, University of Tiaret, Algeria
[2] Laboratoire de Technologie des Matériaux, USTHB, Algiers, Algeria
E-mail: yassine.elguerri@univ-tiaret.dz

In this study, a single-phase boride layer thickness Fe_2B is predicted on two different substrates (Armco iron and XC38 steel) by following the integral method. This method is a mathematical model based on a system of differential algebraic equations that help to deduce the diffusion coefficient, which is the key factor on predicting the layer thickness. Literatures cover different diffusion coefficients for each substrate, albeit researchers usually extract from experimental data, variations of growth rate constants within only one time treatment and deduce the diffusion coefficient from them. This deduction is done via an estimation of a frequency factor and an activation energy from the growth rate constants. Therefore, our main aim is to illustrate the impact of the deduction of the diffusion coefficient on predicting the boride layer thickness. Lastly, the impact with and without incubation time on the boriding kinetics of both substrates was also examined.

INTRODUCTION

Lifespan of machine parts and tools is one of the most important factors for factories due to their exposure to wear during the use in machining or any other purpose. In order to enhance their wear resistance, engineers studied surface properties and have presented different surface hardenings, one of them is the boriding process, also known as boronizing.

Boriding is a thermo-chemical treatment based on the diffusion of boron atoms at high temperatures into metals forming a boride layer. Such a layer can be either monophase or multiphase and is extremely hard. It increases abrasive, adhesion and corrosion wears, thus improving tribological properties [1] and raising the material's lifespan expectancy by three to ten times [2].

This process can be carried out in solid, liquid and gaseous media [3,4]. Nevertheless, solid ones as from powder mixtures like powder pack boriding are more favored and more frequently used due to the simplicity of their technology and economic advantages [5]. The process is more suited on carbon and low alloyed steels but can also be applied to other metal-based materials [6,7]. Carbon steels boriding is usually carried out at temperatures ranging from 800 to 1050 °C for treatment times of 1 to 12 hours [8] giving a characteristic saw-toothed surface morphology consisting of either a single-phase iron boride Fe_2B or bi-phased iron borides FeB and Fe_2B [3]. The single-phased layer is more favored than the bi-phased one and that's explained from even though FeB is in theory harder with a Vickers Hardness of 1800 to 2100 HV than Fe_2B with a range of 1400 to 1600 HV, it is generally unwanted due to its brittleness [2,9] which when high loads are applied, high stresses and crack formations appear along the FeB/Fe_2B interface. In addition, the borides FeB and Fe_2B have two different coefficients of thermal expansion, thus during the treatment, spalling is observed in the bi-phased layer [10].

Researchers have developed several approaches in order to model boriding kinetics for steels [11-15], cast iron [16,17] and Armco iron [18-22]. One of those researches, the integral method, a mathematical model that predicts the boride layer thickness based upon certain parameters like temperature, time treatment, boron concentrations in the boride phases.

This study uses an approach based on the integral method [22] to determine the most important factor in the boriding process which is the boron diffusion coefficient. It is deduced from the kinetic data, considered as the main variable required for predicting the boride layer thickness. Researchers deduce it differently based upon a certain time treatment [22-24] and those differences have an impact on the predictions' accuracy.

Furthermore, the incubation time was overlooked, firstly, to see that impact in simpler terms, secondly, to evaluate if overlooking has itself an important impact on the predictions.

INTEGRAL METHOD

Symbols

u – boride layer thickness;
u_{exp} – experimental boride layer thickness;
u_{pre} – predicted boride layer thickness;
k – growth rate constant;
t – boride treatment time;
t_0 – incubation time;
C_{ads} – adsorbed boron concentration;
$C_{up}^{Fe_2B}$ – upper boron concentration of the layer;
$C_{low}^{Fe_2B}$ – lower boron concentration of the layer;
C_0 – solubility limit of boron within the substrate;
T – absolute temperature;
D – boron diffusion coefficient;
D_0 – frequency factor;
Q – activation energy.

Model

The integral method is a mathematical model developed to describe the growth of the boride layer formed on top of the substrate. The distribution of boron concentration across the Fe_2B boride layer is illustrated schematically in Figure 1.

In the beginning of the boriding process, the boron atoms penetrate into the lattice of the substrate by thermo diffusion and after a period called incubation time t_0, a saturated solid solution is formed and the treatment time t begins with the formation of a continuous and more compact Fe_2B boride layer having a thickness u. C_{ads} denotes the absorbed boron concentration at material surface [10]. C_0 is the solubility limit of boron within the material substrate which can be neglected (≈ 0 wt.%) [25,26].

To establish this diffusion model, certain assumptions are considered.

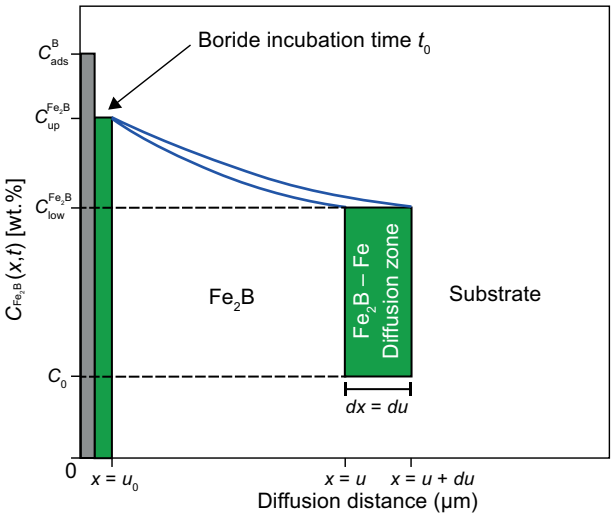


Fig. 1. Boron concentration profile across the Fe_2B boride layer

• Initial condition:

$$\text{at } t = 0, x > 0 \text{ we have } C_{Fe_2B} = C_0 \tag{1}$$

• Boundary conditions:

$$\text{when } x = 0,\ t = t_0 \quad \text{we have } C_{Fe_2B} = C_{up}^{Fe_2B} \text{ for } C_{ads} > C_{low}^{Fe_2B} \tag{2}$$

$$\text{when } x = u,\ t = t \quad \text{we have } C_{Fe_2B} = C_{low}^{Fe_2B} \text{ for } C_{ads} < C_{low}^{Fe_2B} \tag{3}$$

The boron concentration profile is described by Fick's second law, a partial differential equation (PDE) that predicts how diffusion causes the concentration to change with respect to time:

$$\frac{\partial C_{Fe_2B}}{\partial t} = D_B^{Fe_2B} \frac{\partial^2 C_{Fe_2B}}{\partial x^2} \tag{4}$$

where the boron diffusion coefficient is only dependent on the boriding temperature, $D_B^{Fe_2B}(T)$.

The expression of boron concentration profile throughout the boride layer can be obtained using the Goodman's method (HBIM) [27].

$$C_{Fe_2B}(x, t) = C_{low}^{Fe_2B} + a(t)\,[u(t) - x] + b(t)\,[u(t) - x]^2 \tag{5}$$

where the boron concentration inside the boride layer adopts a certain shape that depends on $a(t)$, $b(t)$ and $u(t)$ which are three time-dependent variables. The first and second variables must be positive due to the decreasing nature of the concentration.

Using the second boundary condition, equation (3), we get the first algebraic equation:

$$C_{up}^{Fe_2B} - C_{low}^{Fe_2B} = a(t)\,u(t) + b(t)\,u(t)^2 \tag{6}$$

By integrating the second Fick's law in a range of 0 to $u(t)$ using Leibniz's law we obtain:

$$\frac{u(t)^2}{2}\frac{da(t)}{dt} + a(t)\,u(t)\frac{du(t)}{dt} + \frac{u(t)^3}{3}\frac{db(t)}{dt} + b(t)\,u(t)^2\frac{du(t)}{dt} = 2D_B^{Fe_2B} b(t)\,u(t) \tag{7}$$

Based on the principle of mass conservation at the (Fe_2B/Substrate) interface, a second algebraic equation can be obtained:

$$W\left.\frac{\partial x}{\partial t}\right|_{x=u} = -D_B^{Fe_2B}\left.\frac{\partial C_{Fe_2B}}{\partial x}\right|_{x=u} \tag{8}$$

with $$W = \frac{C_{up}^{Fe_2B} + C_{low}^{Fe_2B} - 2C_0}{2} \tag{9}$$

The previous equation is rewritten to the following form:

$$W\left(\frac{\left.\frac{\partial C_{Fe_2B}}{\partial t}\right|_{x=u}}{\left.\frac{\partial C_{Fe_2B}}{\partial x}\right|_{x=u}}\right) = -D_B^{Fe_2B}\left.\frac{\partial C_{Fe_2B}}{\partial x}\right|_{x=u} \tag{10}$$

After derivations and some mathematical manipulations, we obtain the third and last algebraic equation:

$$(C_{up}^{Fe_2B} + C_{low}^{Fe_2B})\, b(t) = a(t)^2 \tag{11}$$

The three past algebraic equations (6), (7) and (11) form the differential algebraic equations (DAE) system whose unknowns are $a(t)$, $b(t)$ and $u(t)$. That DAE system can finally be solved either analytically [13, 28, 29] or numerically [30]. Going with the analytical approach, a feasible solution is set as:

$$u(t) = k\sqrt{t - t_0} \tag{12}$$

$$a(t) = \frac{\alpha}{u(t)} \tag{13}$$

$$b(t) = \frac{\beta}{u(t)^2} \tag{14}$$

In our approach, we'll overlook the incubation time t_0, assuming that it is nonexistent as if we didn't have the equipment to measure it. Then, Equation (12) can be rewritten as:

$$u(t) = k\sqrt{t} \tag{15}$$

By substituting the expressions of time-dependent parameters $a(t)$ and $b(t)$ into equation (6) and (11), the following algebraic equations are obtained:

$$C_{up}^{Fe_2B} + C_{low}^{Fe_2B} = \alpha + \beta \tag{16}$$

$$(C_{up}^{Fe_2B} + C_{low}^{Fe_2B})\, \beta = \alpha^2 \tag{17}$$

By then, we can resolve this algebraic system of equations (16) and (17) to determine the two unknown parameters, α and β, that are the possible solutions.

$$\alpha = (C_{up}^{Fe_2B} + C_{low}^{Fe_2B})\left[-1 + \sqrt{1 + 4\left(\frac{C_{up}^{Fe_2B} - C_{low}^{Fe_2B}}{C_{up}^{Fe_2B} + C_{low}^{Fe_2B}}\right)}\right]/2 \tag{18}$$

$$\text{with} \quad \beta = (C_{up}^{Fe_2B} + C_{low}^{Fe_2B})\left[2 + 4\left(\frac{C_{up}^{Fe_2B} - C_{low}^{Fe_2B}}{C_{up}^{Fe_2B} + C_{low}^{Fe_2B}}\right) - 2\sqrt{1 + 4\left(\frac{C_{up}^{Fe_2B} - C_{low}^{Fe_2B}}{C_{up}^{Fe_2B} + C_{low}^{Fe_2B}}\right)}\right]/4 \tag{19}$$

Substituting the analytic solution equations into equation (7) and derivation with respect to time, equation (20) is deduced [22].

$$D_B^{Fe_2B} = \eta k^2 \tag{20}$$

with

$$\eta = \frac{1}{12} + \frac{1}{16}\,\frac{C_{up}^{Fe_2B} + C_{low}^{Fe_2B}}{C_{up}^{Fe_2B} - C_{low}^{Fe_2B}}\left[1 + \sqrt{1 + 4\left(\frac{C_{up}^{Fe_2B} - C_{low}^{Fe_2B}}{C_{up}^{Fe_2B} + C_{low}^{Fe_2B}}\right)}\right] \tag{21}$$

Finally, the three time-dependent parameters $a(t)$, $b(t)$ and $u(t)$ are attained analytically and expressed as follows:

$$a(t) = (C_{up}^{Fe_2B} + C_{low}^{Fe_2B})\left[-1 + \sqrt{1 + 4\left(\frac{C_{up}^{Fe_2B} - C_{low}^{Fe_2B}}{C_{up}^{Fe_2B} + C_{low}^{Fe_2B}}\right)}\right]/2\,k\sqrt{t} \tag{22}$$

$$b(t) = (C_{up}^{Fe_2B} + C_{low}^{Fe_2B})\left[2 + 4\left(\frac{C_{up}^{Fe_2B} - C_{low}^{Fe_2B}}{C_{up}^{Fe_2B} + C_{low}^{Fe_2B}}\right) - 2\sqrt{1 + 4\left(\frac{C_{up}^{Fe_2B} - C_{low}^{Fe_2B}}{C_{up}^{Fe_2B} + C_{low}^{Fe_2B}}\right)}\right]/4\,k^2 t \tag{23}$$

$$u(t) = \sqrt{\frac{D_B^{Fe_2B}\, t}{\eta}} \tag{24}$$

EXPERIMENTAL DATA

Two kinetics data were used in the present study regarding the thicknesses of Fe_2B layers on two substrates (Armco iron and XC38 Steel):

Figure 2 gives the experimental Fe_2B layer thickness versus the treatment times at 850 °C, 900 °C, 950 °C and 1000 °C for the Armco iron [20] while Figure 3 describes the time dependence of Fe_2B layer thickness at increasing temperatures in case of the XC 38 steel [23]. The lower boron concentration was for both substrates $C_{low}^{Fe_2B}$ = 8.83 wt.% and the upper boron concentration was $C_{up}^{Fe_2B}$ = 9.00 wt.% for the Armco iron and $C_{up}^{Fe_2B}$ = = 8.91 wt.% for the XC38 Steel.

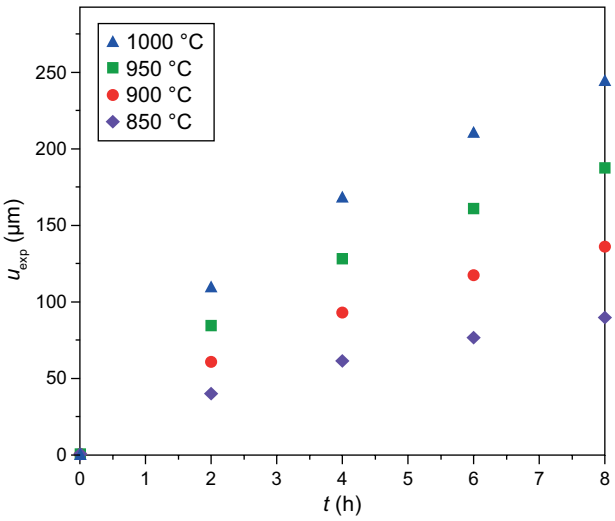


Fig. 2. Experimental boride layer thicknesses over treatment time at different boriding temperatures on the Armco iron substrate [20]

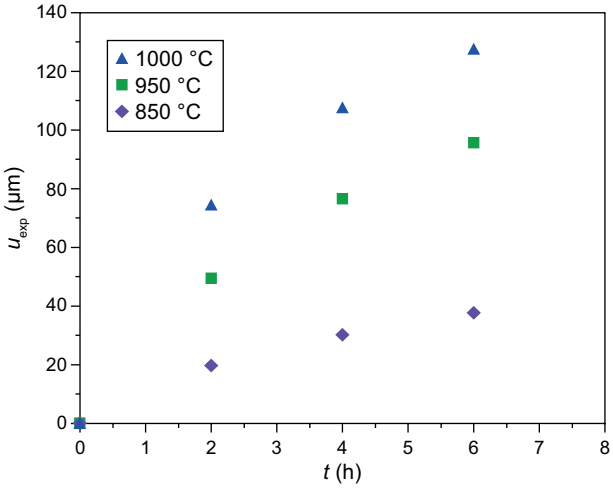


Fig. 3. Experimental boride layer thicknesses over treatment time at different boriding temperatures on the XC38 Steel [23]

CALCULATION STEPS

The following steps will be used on the Armco iron substrate which is the first experimental data set.

Extracting growth rate constants

Using the equation (15), the growth rate constant k was calculated based on the experimental data of the layer thickness u and treatment time t.

Tab. 1. The set of growth rate constants

k [µm s$^{-0.5}$]					
T [°C]	t [h]				
	k_T^{2h}	k_T^{4h}	k_T^{6h}	k_T^{8h}	k_T^{mean}
850	0.4754	0.5123	0.5241	0.5299	0.5104
900	0.7198	0.7772	0.7953	0.8043	0.7742
950	0.9911	1.0683	1.0927	1.1047	1.0642
1000	1.2901	1.3903	1.4223	1.4379	1.3852

Note: that k_{mean} is the mean of each temperature's growth rates.

$$D_T^{mean} = \frac{\sum_{i=t}^{n} k_T^i}{\eta} \tag{25}$$

where n denotes the number of experiments at each temperature, T is the boriding temperature and for each experiment i = 2 h, 4 h, 6 h... as in our data for example.

Diffusion coefficient deduction

The deduction of the diffusion coefficient $D_B^{Fe_2B}$ is the key step of our work. To deduce it, equation (20) is used, but to do so, a choice of a set of growth rate constants is done. As shown in Tab. 1 we have either k_T^{2h}, k_T^{4h}, k_T^{6h}, k_T^{8h} or k_T^{mean}.

Generally, researchers see how the growth rate constant k varies with different temperatures T for the same time treatment t [22-24], taking for example the layer thickness u for a time treatment t of 2 h with different temperatures T and getting from it the growth rate constants k, which means in a nutshell, choosing k_T^{2h}. That choice of k_T^{2h} over the others makes them deduce different diffusion coefficients D, and since the whole method is based upon it, different deductions impact the prediction of the boride layer thickness u. Hence our approach focuses on the k_T^{mean} for accuracies reasons.

Following the integral method, after replacing the upper and lower boron concentrations at the considered interface $C_{up}^{Fe_2B}$ = 9.00 wt.%, $C_{low}^{Fe_2B}$ = 8.83 wt.% in equation (21) we get η = 13.3175. Using it and the chosen set of growth rate constants k_T^i in equation (20) we get the diffusion coefficient D_T^i.

To make an equation for these variations of the diffusion coefficient with respect to the temperature $D(T)$, we used the equation of Arrhenius [8] which in the same time estimates the frequency factor D_0 and the activation energy Q.

$$D(T) = D_0\, e^{-(Q/RT)} \tag{26}$$

where that R is the universal gas constant equals to 8.314 J.mol^{-1} K^{-1}.

Equation (26) can be rewritten in a linear form giving us equation (27).

$$\ln D = -(Q/R)\cdot(1/T) + \ln D_0 \tag{27}$$

Using that equation (27) with the values we had of D_T^{2h}, we get a graph of the natural logarithm of the

Tab. 2. Diffusion coefficients calculated from the set of growth rate constants obtained from two hours of treatment time at different temperatures.

T [°C]	850	900	950	1000
k_T^{2h} [m s$^{-0.5}$]	0.4754 E-6	0.7198 E-6	0.9911 E-6	1.2901 E-6
D_T^{2h} [m s$^{-0.5}$]	03.0100 E-12	06.9006 E-12	13.0822 E-12	22.1656 E-12

diffusion coefficient versus the inverse of temperature ln D (1/T) as illustrated in Figure 4. This graph helps to easily estimate the frequency factor and the activation energy .

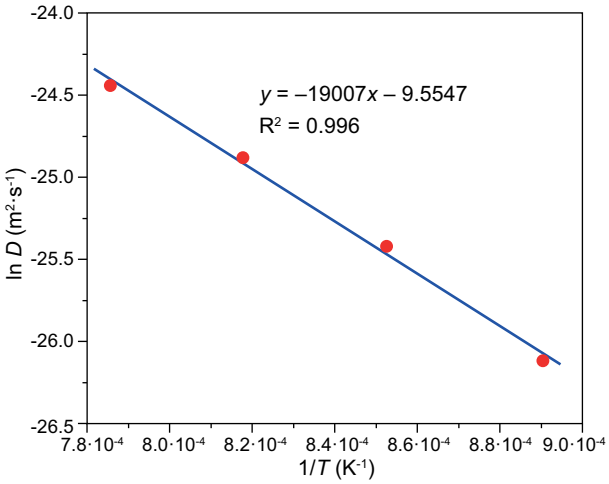


Fig. 4. Diffusion coefficient's natural logarithm as a function of inverse of temperature from a treatment time of two hours

Using a linear regression, the estimations were D_0 = = 7.0870 E-05 m² s⁻¹ and Q = 158.0266 E+03 J mol⁻¹; deducing in the end the equation that gives the diffusion coefficient's value depending on the temperature $D_B^{Fe_2B}(T)$, equation (28).

$$D_T^{2h} = 7.0870 \times 10^{-5}\, e^{-(158.0266\times 10^3/RT)} \quad (28)$$

The deduction step is repeated for k_T^{4h}, k_T^{6h}, k_T^{8h} and k_T^{mean}, in order to estimate five different frequency factors D_0 and activation energies Q from which we get five different equations D_T^{2h}, D_T^{4h}, D_T^{6h}, D_T^{8h} and D_T^{mean} for the diffusion coefficient $D_B^{Fe_2B}$, each using a deduction process.

$$D_T^{4h} = 8.1806 \times 10^{-5}\, e^{-(157.9562\times 10^3/RT)} \quad (29)$$

$$D_T^{6h} = 8.5565 \times 10^{-5}\, e^{-(157.9500\times 10^3/RT)} \quad (30)$$

$$D_T^{8h} = 8.7262 \times 10^{-5}\, e^{-(157.9263\times 10^3/RT)} \quad (31)$$

$$D_T^{mean} = 8.1246 \times 10^{-5}\, e^{-(157.9632\times 10^3/RT)} \quad (32)$$

Prediction of boride layer thickness

After we have deduced the diffusion coefficients D_T^{2h}, D_T^{4h}, D_T^{6h}, D_T^{8h} and D_T^{mean}, replacing each of them separately into equation (24) gives us different predicted Fe_2B boride layer thicknesses, u_{pre}^{2h}, u_{pre}^{4h}, u_{pre}^{6h}, u_{pre}^{8h} and u_{pre}^{mean} as illustrated in Figure 5 and Table 3.

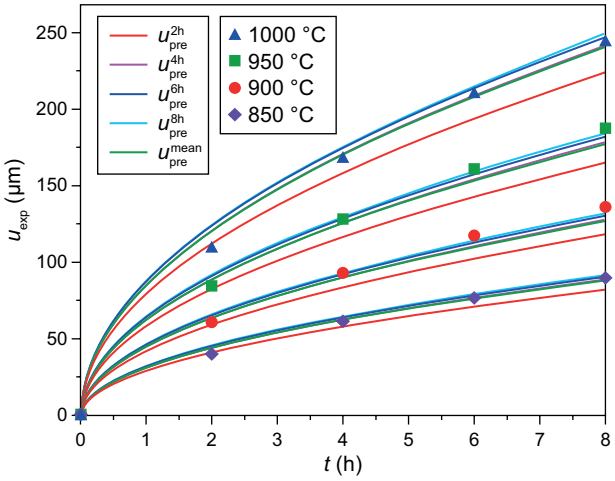


Fig. 5. Predicted boride layer thicknesses over time for different temperatures in case of Armco iron substrate using different deduced diffusion coefficients

Tab. 3. Numerical predicted boride layer thicknesses over time for different temperatures in case of Armco iron substrate based on different deduced diffusion coefficients

u_{pre}^{i} [µm]	T [°C]	t [h]			
		2	4	6	8
u_{pre}^{2h}	850	41.34	58.46	71.60	82.68
	900	59.30	83.86	102.71	118.59
	950	82.58	116.79	143.04	165.16
	1000	112.06	158.47	194.09	224.11
u_{pre}^{4h}	850	44.58	63.05	77.22	89.17
	900	63.94	90.42	110.74	127.88
	950	89.03	125.91	154.21	178.07
	1000	120.79	170.83	209.22	241.59
u_{pre}^{6h}	850	45.61	64.50	79.00	91.22
	900	65.41	92.51	113.30	130.82
	950	91.08	128.81	157.76	182.17
	1000	123.57	174.76	214.04	247.15
u_{pre}^{8h}	850	46.12	65.22	79.88	92.24
	900	66.14	93.53	114.55	132.27
	950	92.09	130.23	159.50	184.18
	1000	124.93	176.68	216.39	249.87
u_{pre}^{mean}	850	44.41	62.81	76.93	88.83
	900	63.70	90.08	110.32	127.39
	950	88.70	125.44	153.63	177.39
	1000	120.34	170.19	208.43	240.68

Calculating errors

To see the impact of those different diffusion coefficients deduced, we calculated the errors between each of the predicted boride layer thickness results and the

experimental data $Errors_{pre}^{i}$ using the standard error of the estimate SEE, with equation (33), the mean absolute error MAE, with equation (34), the minimal/maximal errors and SEE_t which denotes the standard error of the estimate within the same treatment time t. The obtained results were represented in Figure 6 and Table 4 below:

$$SEE = \sqrt{\frac{\sum_{i=1}^{n}(u_i - \bar{u})^2}{n-2}} \tag{33}$$

$$MAE = \frac{1}{n}\sum_{i=1}^{n}|u_i - \bar{u}| \tag{34}$$

where u_i denotes the predicted value, $\bar{u}$ is the actual value and n the number of predictions.

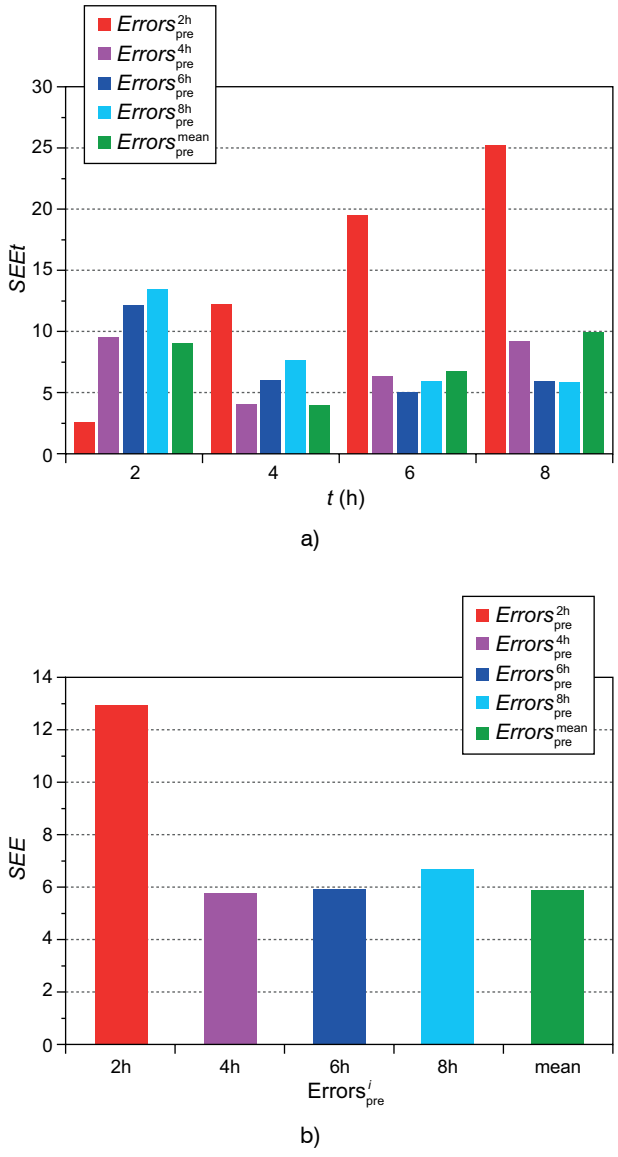


Fig. 6. Diagram of the SEE within each treatment time (a) and for each approach's predictions (b) on the Armco iron substrate

Tab. 4. Numerical predicted boride layer thicknesses over time for different temperatures in case of Armco iron substrate based on different deduced diffusion coefficients

	$Errors^{i}_{pre}{}^{2h} = u^{i}_{pre}{}^{2h} - u_{exp}$				
$Errors_{pre}^{2h}$	**850 °C**	1.00	-3.02	-5.42	-7.24
	900 °C	-1.78	-9.40	-14.18	-17.90
	950 °C	-1.52	-11.40	-17.56	-22.32
	1000 °C	2.59	-8.37	-14.94	-19.91
	SEEt	2.57	12.20	19.52	25.17
	SEE	12.93			
	MAE	9.91			
	Err	min	1.00	22.32	max
$Errors_{pre}^{4h}$	**850 °C**	4.24	1.57	0.20	-0.75
	900 °C	2.86	-2.84	-6.15	-8.61
	950 °C	4.93	-2.28	-6.39	-9.41
	1000 °C	11.32	3.99	0.19	-2.43
	SEEt	9.45	3.98	6.27	9.20
	SEE	5.72			
	MAE	4.26			
	Err	min	0.19	11.32	max
$Errors_{pre}^{6h}$	**850 °C**	5.27	3.02	1.98	1.30
	900 °C	4.33	-0.75	-3.59	-5.67
	950 °C	6.98	0.62	-2.84	-5.31
	1000 °C	14.10	7.92	5.01	3.13
	SEEt	12.13	6.03	5.00	5.99
	SEE	5.91			
	MAE	4.49			
	Err	min	0.62	14.10	max
$Errors_{pre}^{8h}$	**850 °C**	5.78	3.74	2.86	2.32
	900 °C	5.06	0.27	-2.34	-4.22
	950 °C	7.99	2.04	-1.10	-3.30
	1000 °C	15.46	9.84	7.36	5.85
	SEEt	13.45	7.59	5.87	5.84
	SEE	6.62			
	MAE	4.97			
	Err	min	0.27	15.46	max
$Errors_{pre}^{mean}$	**850 °C**	4.07	1.33	-0.09	-1.09
	900 °C	2.62	-3.18	-6.57	-9.10
	950 °C	4.60	-2.75	-6.97	-10.09
	1000 °C	10.87	3.35	-0.60	-3.34
	SEEt	9.02	3.92	6.79	9.92
	SEE	5.87			
	MAE	4.41			
	Err	min	0.09	10.87	max

RESULTS AND DISCUSSIONS

Impact of diffusion coefficient deduction

Table 5 below gives what some literatures presented concerning the activation energy for the boron diffusion into the Fe_2B boride layer of the Armco Iron substrate and Table 6 shows ours results.

If we compare these results with those of the literature, we find a good agreement between our value of the activation energy 157.963 kJ mol^{-1} and the other results listed in Table 5. However, as shown in the errors that follows, the small differences have an impact on the predictions, especially in the frequency factor D_0.

The first diagram in Figure 6 and Table 7 illustrate some inaccuracies like, deducing the diffusion coefficient based on 2 hours of treatment time D_T^{2h} impacts the prediction of the boride layer thickness u_{pre}^{2h} leading it to concentrate mainly on the predictions of 2 hours and ignoring others. Hence why, the standard error of the estimate is 2.57 for 2 hours of treatment time which is low compared to the values obtained for 4, 6 and 8 hours that are respectively 12.20, 19.52 and 25.17. Moreover, the finest results between the others were u_{pre}^{4h} and u_{pre}^{mean} due to them having the most balanced standard error of the estimate across all hours. So, if we were to predict the layer thickness at other treatment-times with them, we would be pretty confident with our accuracies.

Table 8 and the second diagram in the Figure 6 summarize all of the inaccuracies in simpler terms and shows very well the impact of deducing the diffusion coefficient D from a certain time treatment over the other on the prediction of the boride layer thickness .

As seen with the overall standard error of the estimate (*SEE*) and the mean absolute error (*MAE*), they are high if we predict the boride layer thickness u_{pre}^{2h} by deducing the diffusion coefficient D_T^{2h} from a treatment time of 2 hours. Even the maximal error (*Max Err*) found in that prediction is well beyond compared to the others.

Tab. 7. Standard error of the estimate within the same treatment time for each approach's predictions on the Armco iron substrate

		t [h]			
		2	**4**	**6**	**8**
SEEt	u_{pre}^{2h}	2.57	12.20	19.52	25.17
	u_{pre}^{4h}	9.45	3.98	6.27	9.20
	u_{pre}^{6h}	12.13	6.03	5.00	5.99
	u_{pre}^{8h}	13.45	7.59	5.87	5.84
	u_{pre}^{mean}	9.02	3.92	6.79	9.92

Tab. 8. SEE, MAE and the min-max errors of each approach's predictions on the Armco iron substrate

	u_{pre}^{2h}	u_{pre}^{4h}	u_{pre}^{6h}	u_{pre}^{8h}	u_{pre}^{mean}
SEE	12.93	5.72	5.91	6.62	5.87
MAE	9.91	4.26	4.49	4.97	4.41
Min *Err*	1.00	0.19	0.62	0.27	0.09
Min *Err*	22.32	11.32	14.10	15.46	10.87

The other thing seen is that the minimum and maximum errors are reduced in the u_{pre}^{mean} compared to others and that confirms the balanced predictions we talked about before.

Overall, the finest result seen with pretty low standard error of the estimate (*SEE*) and mean absolute error (*MAE*) while in the same time having the lowest maximal error (*Max Err*) is the predicted boride layer thickness u_{pre}^{mean} made from the deduction of D_T^{mean}, the diffusion coefficient deduced from our approach which used equation (25) which calculate the mean of the growth rate constants k_T^{mean}.

Tab. 5. Different activation energies depending on the boriding method found in the literature for the Armco iron

Boriding method	**Gaseous**	**Paste**	**Paste**	**Powder**	**Powder**	**Powder**
Activation energy *Q* [kJ mol^{-1}]	120.65	151.00	157.00	157.50	157.9	157.94
References	[31]	[32]	[24]	[20]	[21]	[22]

Tab. 6. Activation energies and frequency factors estimated from the different deduced diffusion coefficients of the Armco iron substrate

Diffusion coefficient *D* [m^2 s^{-1}]	D_T^{2h}	D_T^{4h}	D_T^{6h}	D_T^{8h}	D_T^{8h}
Frequency factor D_0 [m^2 s^{-1}]	7.087 E-5	8.181 E-5	8.557 E-5	8.726 E-5	8.125 E-5
Activation energy *Q* [kJ mol^{-1}]	158.027	157.956	157.950	157.926	157.963

Impact of overlooking incubation time

To see the impact of overlooking incubation time, our results u_{pre}^{mean} which predicts the boride layer thickness without taking into account the incubation time t_0 and the results which did take it into account $u_{pre}^{incubation}$ [22] were plotted in Figure 7.

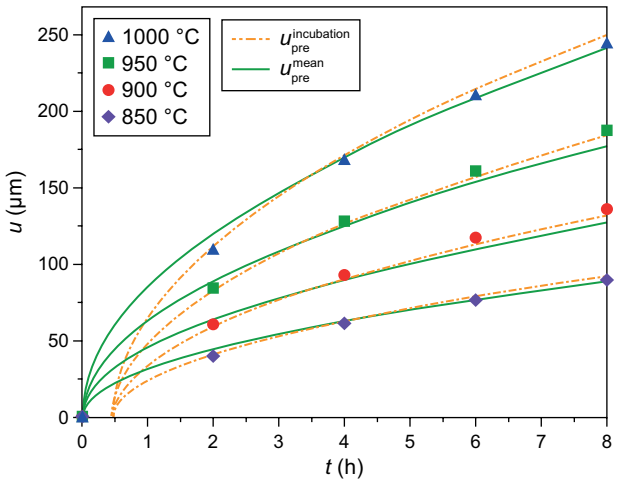


Fig. 7. Predicted boride layer thickness over time at different temperatures with and without the presence of incubation time in case of Armco iron substrate

Figure 7 shows that they both vary parabolically with the treatment time. However, for the predicted layer thicknesses with the incubation time $u_{pre}^{incubation}$, the thickness doesn't increase until the substrate's surface saturates contrary to our predictions u_{pre}^{mean} which didn't take that phenomenon into account. To better see these results, errors of each prediction were given in Table 9.

Tab. 9. *SEE*, *MAE* and the min-max errors of each approach's predictions on the Armco iron substrate in two different scenarios, taking into account the incubation time and overlooking it

	u_{pre}^{mean}	$u_{pre}^{incubation}$
SEE	5.87	3.44
MAE	4.41	2.94
Min Err	0.09	1.06
Max Err	10.87	5.91

So, we can say that even though we overlooked the incubation time t_0, taking all data into account using the mean of the growth rate constants k_T^{mean}, our predictions weren't as bad or as far from experimental data.

To further see our prediction's accuracy, we took another experiment's result with a layer thickness of 175 µm at 980 °C for 5 hours [20] and compared it to the predicted boride layer thickness using our approach which overlooked the incubation time and the approach which considered it [22]. See Tab. 10.

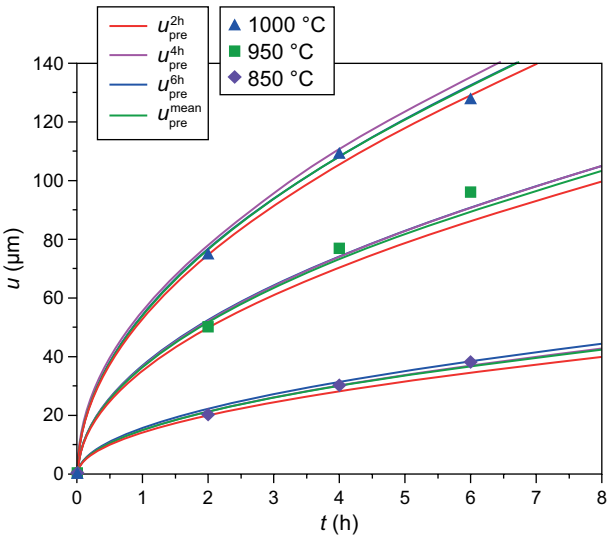
Tab. 10. The absolute error of predicting the boride layer thickness at 980 °C for 5 h with and without the occurrence of boride incubation time

5 h at 980 °C	
u_{exp}	
175 ± 12	
u_{pre}^{mean}	$u_{pre}^{icubation}$
169.09	179.79
Absolute Error	
6.09	4.79

After this, we can confirm that even though we overlooked the incubation time t_0 in our approach u_{pre}^{mean}, we still had a great prediction, close to the other study which considered it $u_{pre}^{incubation}$.

Validating impacts

To validate our approach, and the impacts seen, we've used it on an entirely other substrate XC38 steel. Figure 8 and Table 11 compare between the values of experimental layers' thicknesses found in the second data set [23] and the predicted results of our approach with the associated errors of computation for XC38 steel.



a)

Fig. 8. Predicted boride layer thicknesses over time in different temperatures and their SEE on the XC38 steel substrate using different deduced diffusion coefficients *(Continue on next page)*

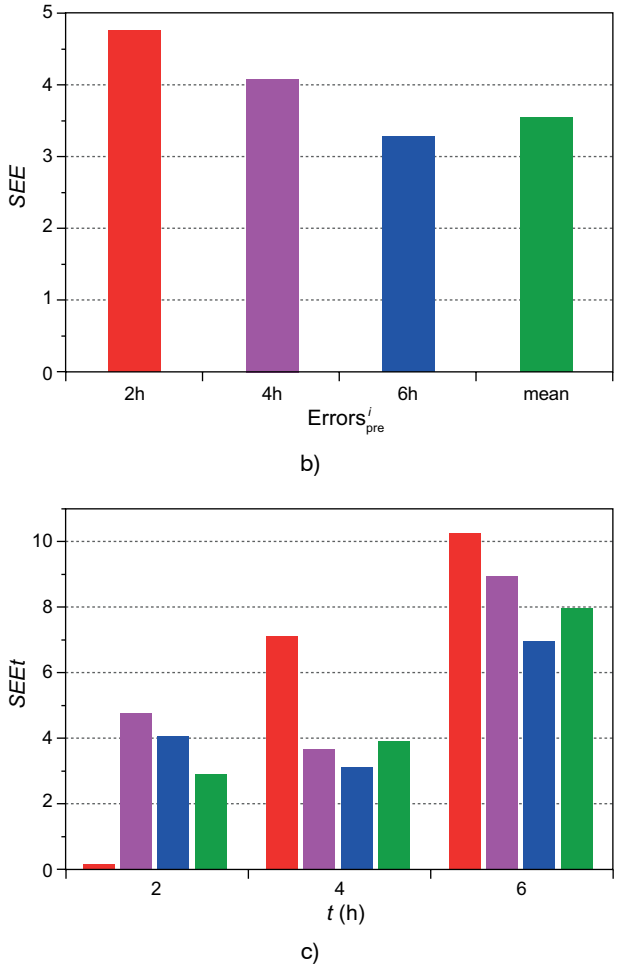


Fig. 8. Predicted boride layer thicknesses over time in different temperatures and their SEE on the XC38 steel substrate using different deduced diffusion coefficients

As seen with the other substrate, the different deductions of the diffusion coefficient $D_B^{Fe_2B}$ have an impact on predicting the boride layer thickness. Therefore, the approach of taking the mean of the growth rate constants k_T^{mean} using equation (25) leads to the finest predictions u_{pre}^{mean} without needing to calculate the others. Hence, it allowed us to validation of the first impact.

After that, we compared our results' approach u_{pre}^{mean} with the results that considered the incubation time and with a totally different method than the integral method, $u_{pre}^{incubation}$, found in [23]. The results were illustrated in Figure 9 and the difference between them is better seen numerically in term of errors on Table 12.

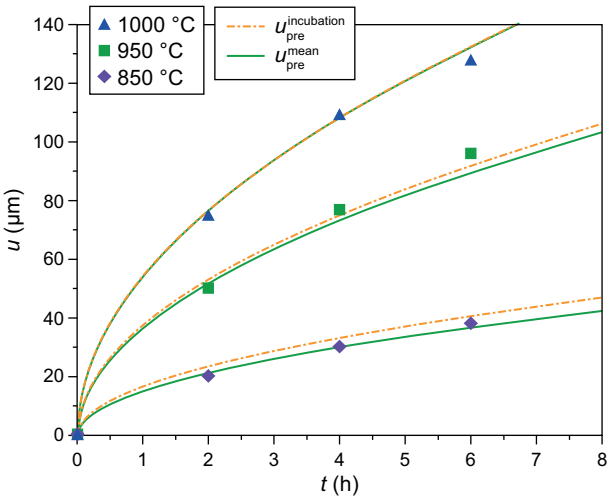


Fig. 9. Predicted boride layer thickness over time at different temperatures with and without the incubation time on the XC38 steel

Tab. 12. *SEE*, *MAE* and min-max errors of each approach's predictions in case of borided XC38 steel with and without the incubation time

	u_{pre}^{mean}	$u_{pre}^{incubation}$
SEE	3.53	3.46
MAE	2.37	2.81
Min Err	0.05	0.44
Max Err	6.46	4.82

Tab. 11. Details about each approach's predictions on the XC38 steel substrate

		u_{pre}^{2h}			u_{pre}^{4h}			u_{pre}^{6h}			u_{pre}^{mean}		
D_T^i	D_0 [m^2 s^{-1}]	3.719 E-3			2.950 E-3			1.171 E-3			2.327 E-3		
	Q [kJ mol^{-1}]	208.549			205.091			195.736			203.053		
SEEt		***t* [h]**			***t* [h]**			***t* [h]**			***t* [h]**		
		2	4	6	2	4	6	2	4	6	2	4	6
		0.17	7.12	10.24	4.75	3.67	8.93	4.07	3.13	6.97	2.92	3.90	7.98
SEE		4.71			4.07			3.27			3.53		
MAE		2.78			2.93			2.46			2.37		
Min Err		0.01			0.31			0.45			0.05		
Max Err		9.60			7.44			4.99			6.46		

Second impact validated too; Even though we overlooked the incubation time t_0, we have predicted the boride layer thickness pretty accurately as well, with 2.37 of mean absolute error, better than the study that took into consideration the incubation time with 2.81 of mean absolute error [23].

CONCLUSIONS

The diffusion coefficient is the main factor impacting the predictions' accuracies when studying the kinetics growth of Fe_2B boride layers' thicknesses. Its deduction is influenced by the choice of the set of growth rate constants. As elucidated in the first impact.

Our developed approach overlooked the incubation time and was based on using the mean set of growth rate constants including all experimental data. It helped to deduce the mean diffusion coefficient's equation, leading us in the end to the finest boride layer thickness predictions without choosing a set of growth rate constants over the other as explained in the second step.

The second impact concluded was, even though overlooking the incubation time lessen a bit the predictions' accuracy, our approach's predictions were pretty accurate, even comparable when it came to the second substrate's study which took it into account.

The use of two different substrates (Armco iron and XC38 steel) helped in confirming our approach and its conclusions on predicting the growth kinetics of Fe_2B boride layer thickness. Our approach can also be extended to the dual phase boride layer (FeB and Fe_2B).

REFERENCES

1. Tsipas D.N., Rus J., Boronizing of alloy steels, *Journal of Material Science Letter* **1987**, 6, 118-120.
2. Stewart K., Boronizing protects metals against wear, *Advanced Materials & Processes* **1997**, 151(3), 23-25.
3. Kulka M., Current Trends in Boriding Techniques, *Springer* **2019**, 1-8.
4. Davies J.A., Wilbur P.J., Williamson D.I., Wei R., Vajo J.J., Ion implantation boriding of iron and AISI M2 steel using a high-current density, low energy, broad-beam ion source, *Surface and Coatings Technology* **1998**, 103-104, 52-57.
5. Keddam M.S., Chentouf M., A diffusion model for describing the bilayer growth (*FeB/Fe_2B*) during the iron powder-pack boriding, *Applied Surface Science* **2005**, 252, 393-399.
6. Sen S., Sen U., Bindal C., An approach to kinetic study of borided steels, *Surface and Coatings Technology* **2005**, 191(2), 274-285.
7. Von Matuschka A.G., Borieren, *Carl Hanser Verlag München*, Wien **1977**.
8. Milinovi A., Krumes D., Marković R., An investigation of boride layers growth kinetics on carbon steels, *Tehnicki vjesnik* **2012**, 19(1), 27-31.
8. Genel K., Boriding kinetics of H13 steel, *Vacuum* **2006,** 80(5), 451-457.
10. Yu L.G.; Chen X.J.; Khor K.A., Sundararajan G., *FeB/Fe_2B* phase transformation during SPS pack-boriding: Boride layer growth kinetics, *Acta Materialia* ***2005,*** 53(8), 2361-2368.
11. Campos-Silva I.E., Rodríguez-Castro G.A., Boriding to improve the mechanical properties and corrosion resistance of steels, in: E.J. Mittemeijer and M.A.J. Somers (eds.), Thermochemical Surface Engineering of Steels, *Woodhead-Elsevier Publishing, Cambridge* **2015**, 651-697.
12. Zuno-Silva J., Ortiz-Domínguez M., Keddam M., Elias-Espinosa M., Damián-Mejía O., Cardoso-Legorreta E., Abreu-Quijano M., Boriding Kinetics of *Fe_2B* Layers Formed on AISI 1045 Steel, *Journal of Mining and Metallurgy, Section B: Metallurgy* **2014**, 50(2), 101-107.
13. Keddam M., Elias-Espinosa M., Ortiz-Domínguez M., Simón-Marmolejo I., Zuno-Silva J., Pack-boriding of AISI P20 steel: Estimation of boron diffusion coefficients in the *Fe_2B* layers and tribological behaviour, *International Journal of Surface Science and Engineering* **2017**, 11(6), 563-585.
14. Villa Velázquez-Mendoza C.I., Rodríguez-Mendoza J.L., Ibarra-Galván V., Hodgkins R.P., López-Valdivieso A., Serrato-Palacios L.L., Leal-Cruz A.L., Ibarra-Junquera V., Effect of substrate roughness, time and temperature on the processing of iron boride coatings: experimental and statistical approaches, *International Journal of Surface Science and Engineering* **2014**, 8(1) 71-91.
15. Campos I., Islas M., González E., Ponce P., Ramírez G., Use of fuzzy logic for modeling the growth of *Fe_2B* boride layers during boronizing, *Surface and Coatings Technology* **2006**, 201, 2717-2723.
16. Keddam M., A diffusion model for the *Fe_2B* layers formed on a ductile cast iron, *Acta Physica Polonica A* **2018**, 133, 1174-1177.
17. Keddam M., Chegroune R., A Model for Studying the Kinetics of the Formation of *Fe_2B* Boride Layers at the Surface of a Gray Cast Iron, *Applied Surface Science* **2010**, 256, 5025-5030.
18. Ramdan R.D., Takaki T., Tomita Y., Free energy Problem for the Simulations of the Growth of *Fe_2B* Phase Using Phase-Field Method, *Material Transaction* **2008**, 49, 2625-2631.
19. Nait Abdellah Z., Keddam M., Chegroune R., Bouarour B., Haddour L., Elias A., Simulation of the boriding kinetics of *Fe_2B* layers on iron substrate by two approaches, *Matériaux et Techniques* **2012**, 100, 581-588.
20. Elias-Espinosa M., Ortiz-Domínguez M., Keddam M., Flores-Rentería M.A., Damián-Mejía O., Zuno-Silva J., Hernández-Ávila J., Cardoso-Legorreta E., Arenas-Flores A., Growth kinetics of the *Fe_2B* layers and adhesion on Armco iron substrate, *Journal of Materials Engineering and Performance* **2014**, 23, 2943-2952.
21. Keddam M., Kulka M., Mean diffusion coefficient method in studying Armco iron boriding kinetics, *Metal Science and Heat Treatmen* 2020, 62, 5-6.
22. Keddam M., Kulka M., Analysis of the growth kinetics of *Fe_2B* layers by the integral method, *Journal of Mining and Metallurgy, Section B: Metallurgy* **2018**, 54(3), 361-367.
23. Mebarek B., Benguelloula A., Zanoun A., Effect of Boride Incubation Time During the Formation of *Fe_2B* Phase, *Materials Research* **2018**, 21(1), 1-7.

24. Campos-Silva I., Ortiz-Domínguez M., Cimenoglu H., Escobar-Galindo R., Keddam M., Elías-Espinosa M., López-Perrusquia N., Diffusion Model for Growth of Fe_2B Layer in Pure Iron, *Surface Engineering* **2011**, 27, 189-195.
25. Krukovich M.G., Prusakov B.A., Sizov I.G., The Components and Phases of Systems 'Boron-Iron' and 'Boron-Carbon-Iron', Chapter Plasticity of Boronized Layers, *Springer series, Materials Science* **2016**, 237, 13-21.
26. Okamoto H., B-Fe (boron-Iron), *Journal of Phase Equilibria and Diffusion* 25 (2004) 297–298.
27. T.R. Goodman, Application of Integral Methods to Transient Nonlinear Heat Transfer, *Advances in Heat Transfer* **1964**, 1, 51-122.
28. Keddam M., Ortiz-Dominguez M., Elias-Espinosa M., Arenas-Flores A., Zuno-Silva J., Zamarripa-Zepeda D., Gomez-Vargas O.A., Kinetic Investigation and Wear Properties of Fe_2B Layers on AISI 12L14 Steel, *Metallurgical and Material Transaction A* **2018**, 49, 1895-1907.
29. Zuno-Silva J., Keddam M., Ortiz-Domínguez M., Elias-Espinosac M.C., Cervantes-Sodi F., Oseguera-Peña J., De-Dios L.D.F., Gomez-Vargas O.A., Kinetics of formation of Fe_2B layers on AISI S1 steel, *Materials Research* **2018**, 21(5), 1-10.
30. Ascher U., Petzold L., Computer Methods for Ordinary Differential Equations and Differential Algebraic Equations, *SIAM,* Philadelphia **1998**.
31. Keddam M., Kulka M., Makuch N., Pertek A., Małdziński L., A Kinetic Model for Estimating the Boron Activation Energies in the *FeB* and Fe_2B Layers During the Gas-Boriding of Armco Iron: Effect of Boride Incubation Times, *Applied Surface Science* **2014**, 298, 155-163.
32. Campos I., Oseguera J., Figueroa U., García J.A., Bautista O., Kelemenis G., Kinetic study of boron diffusion in the paste-boriding process, *Materials Science and Engineering A* **2003**, 352, 261-265.